

Constructing Low-Triplet-Energy Hosts for Highly Efficient Blue PHOLEDs: Controlling Charge and Exciton Capture in Doping Systems

Chunmiao Han,^{†,‡} Fangchao Zhao,^{†,§} Zhen Zhang,[‡] Liping Zhu,[§] Hui Xu,^{*,‡} Jing Li,[‡] Dongge Ma,^{*,§} and Pengfei Yan[‡]

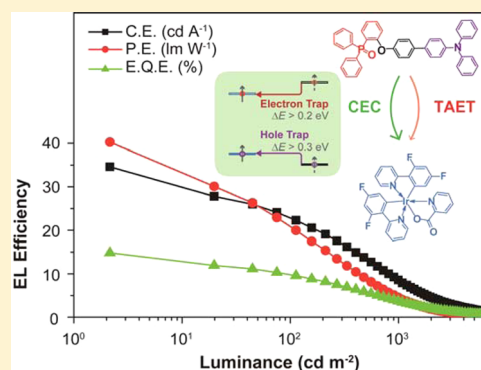
[†]Key Laboratory of Functional Inorganic Material Chemistry, Ministry of Education, Heilongjiang University, 74 Xuefu Road, Harbin 150080, P. R. China

[§]State Key Laboratory of Polymer Physics and Chemistry, Changchun Institute of Applied Chemistry, Chinese Academy of Sciences, Changchun 130022, P. R. China

Supporting Information

ABSTRACT: With the aim to rationally figure out the significance of charge and exciton capture in the electrophosphorescent processes in low-triplet-energy hosts involved doping systems, the frontier molecular orbital (FMO) energy levels of a series low-triplet-energy hosts with diphenylphosphine oxide (DPPO) and triphenylamine (TPA), collectively named DPE_xPOTPA_n , were successfully and gradually tuned on the basis of their constant triplet energy levels (T_1) of 2.63 eV to get rid of interference from host-dopant energy transfer. It was showed that device efficiencies were directly proportional to the depths of carrier traps formed on the dopants and inversely proportional to the exciton capture ability of the hosts, which were evidenced by the highest external quantum efficiency of $\sim 15\%$ from FIrpic-based PHOLED of DPESPOTPA with the deepest hole and electron traps and the weakest exciton capture ability among DPE_xPOTPA_n . This work not only demonstrated the great advantages and potential of this kind of host materials for low-driving-voltage application but also clarified the determinants of highly efficient low-triplet-energy hosts for blue PHOLEDs, which are consequentially referable for purposeful molecular design.

KEYWORDS: blue electrophosphorescence, low triplet energy host, charge capture, exciton capture, phosphine oxide



1. INTRODUCTION

Efficient utilization of high energy excitons is one of the most important issues for electroluminescence (EL) because of the high sensitivity of these excitons to the various quenching effects.^{1–11} Intuitively, the efficient blue organic light-emitting diodes (OLED) can be achieved through the well-managed material characteristics and device configurations for balanced carrier injection and transportation to emitting layers (EML) and the confinement of excitons on emitters.^{12–16} This arouses the vibrant development of high energy-gap organic semiconductors with both improved electroactivity and optical properties to suppress the nonradiative energy losses during the EL process.^{17–24} Among these materials, hosts for blue phosphorescent OLEDs (PHOLED) are highly focused in recent years because of their typical optoelectronic characteristics for fundamental investigation of the structure–property correlations and the corresponding feasible approaches for controllable and selective modifications.^{4,25,26}

For the sake of breaking through the intrinsic inferiority of blue electrophosphorescence in carrier injection and transportation,²⁷ ambipolar host materials with the high enough first triplet energy levels (T_1) are paid much attention in pursuit of

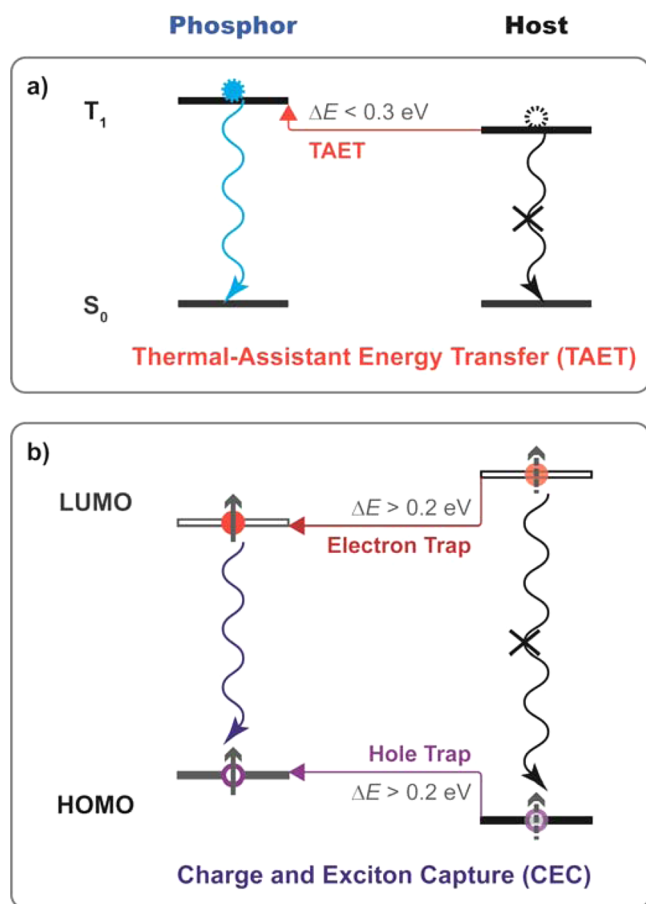
the harmony and unity between low driving voltage and high EL efficiency for portable and low-power applications.^{28–47} Under the conventional strategy, two prerequisites for molecular design should be considered that (i) only groups with high-enough T_1 can be involved,^{48–55} otherwise, the T_1 excited state should be localized on the groups with the high enough T_1 ,^{56,57} (ii) the intermolecular interaction should be carefully restrained to suppress low-energy charge transfer (CT) states and other negative effects.^{32,58–64} Recently, our group developed several novel linkage styles, such as multi-insulating,⁶⁵ indirect and short-axis linkages,^{66,67} to construct a series of high-performance carrier-transporting phosphine oxide (PO) hosts with the focus on achieving high T_1 for low-voltage-driving efficient blue PHOLEDs.⁶⁸ Nevertheless, along with increased complexity of molecular structures, function enhancement and property adjustment are more and more difficult due to the limited utilizable functional groups and linkage styles. This forced us to reconsider the determinants for the molecular

Received: October 6, 2013

Revised: November 24, 2013

design of blue electrophosphorescent host materials. When T_1 of host is equivalent or slightly lower than that of dopant, two main procedures will determine the ultimate exciton availability, viz., (i) energy transfer from host to guest with the thermal assistance^{69–73} and (ii) direct charge capture and exciton recombination on dopant, which are corresponding to optical and electrical procedures, respectively (Scheme 1).^{16,74} Forrest

Scheme 1. Two Key EL Mechanisms for PHOLEDs Involving Low-Triplet-Energy Hosts^a



^a(a) EL mechanism based on thermal-assistant energy transfer (TAET), in which exciton is firstly formed on host with low T_1 and then transferred to phosphor with the thermal assistance to overcome the triplet energy gap. Because energy of thermal fluctuation is less than 0.3 eV at room temperature, the host-dopant triplet energy gap should be within 0.3 eV. (b) Charge and exciton capture (CEC) afforded EL mechanism, in which charge is directly captured by phosphor because of charge traps formed by the FMO energy level differences between host and phosphor and then recombined to afford EL.

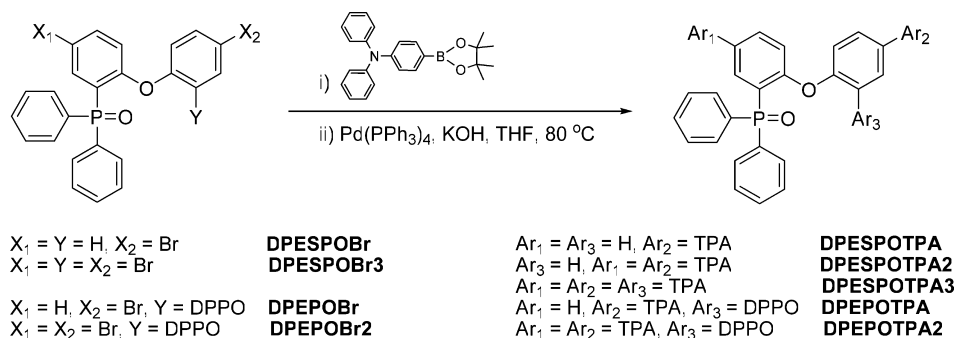
et al. already demonstrated endothermic energy transfer from 4,4'-bis(N-carbazolyl)-1,1'-biphenyl (CBP, $T_1 = 2.56 \text{ eV}$) to bis(4,6-difluorophenylpyridinato- N,C^2)picolinato Iridium(III) (FIrpic, $T_1 = 2.65 \text{ eV}$),⁶⁹ but they just achieved E.Q.E. of only 5% through conventional device configuration. Illuminatingly, the recent work by Padmaperuma et al. reported the achievement of unexpected high E.Q.E. approaching to 14% from CBP-based blue PHOLEDs with FIrpic as the phosphor, ascribed to the well confinement of excitons in EML by the high T_1 of adjacent carrier transporting layers (CTL).⁷⁵ Therefore, it is extremely significant to confirm which one of

these two procedures is dominant. In this case, the explicit insight of one procedure, such as the effects of the electrical characteristics of the hosts on the device performance, without any interference from the other one becomes urgent and imperative. Actually, the deep understanding of the effects and restraints of each single procedure is crucial to guide the future molecular design. In our opinion, the essential condition for achieving high efficiencies through low-triplet-energy hosts should be the exciton confinement on phosphors. In this sense, the charge capture and exciton recombination by the host materials should be suppressed to, in turn, facilitate the similar procedure on dopants.

In this contribution, we rationally utilized the inductive effect of P=O for electrical property adjustment, accompanied with its negligible influence on T_1 , to illustrate the influence of the charge capture and exciton recombination behaviors of low-triplet-energy hosts on the EL performance of FIrpic-based PHOLEDs. A series diphenylphosphine oxide (DPPO)-triphenylamine (TPA) hybrids with low T_1 of 2.63 eV slightly lower than that of FIrpic were prepared, namely 4'-(2-(diphenylphosphoryl)phenoxy)- N,N -diphenylbiphenyl-4-amine (DPESPOTPA), 4'-(4'-(diphenylamino)biphenyl-4-yloxy)-3'-(diphenylphosphoryl)- N,N -diphenylbiphenyl-4-amine (DPESPOTPA2), 1-diphenylamino-4-(2,4-di(diphenylamino)-phenoxy)-5-(diphenylphosphinoyl)-benzene (DPESPOTPA3), 3'-(diphenylphosphoryl)-4'-(2-(diphenylphosphoryl)phenoxy)- N,N -diphenylbiphenyl-4-amine (DPEPOTPA) and 4',4'-oxybis(3'-(diphenylphosphoryl)- N,N -diphenylbiphenyl-4-amine) (DPEPOTPA2), with the collective name as DPE_xPOTPA_n (Scheme 2), in which TPA served as donor (D) to tune the hole injecting/transporting ability and DPPO was involved as acceptor (A) to adjust the electron injecting/transporting ability, accompanied with diphenylether as the bridge. The frontier molecular orbital (FMO) energy levels were successfully modulated through varying functional group ratio, while the negative effects on T_1 were mostly suppressed to result in precisely the same phosphorescence spectra of DPE_xPOTPA_n , which established a feasible platform for the investigation about the influences of electrical characteristics of the hosts on their EL performance without the interference from energy transfer procedure. It indicated that the EL efficiency was grosso modo in direct proportion to the charge trap depth between the host and FIrpic and simultaneously in reverse proportion to the exciton recombination ability of the host. As expected, among these compounds, DPESPOTPA with the deepest charge traps and the weakest exciton recombination ability supported the best blue PHOLEDs with the impressively high efficiencies as 14.8% for E.Q.E. and 40.3 lm W^{-1} for power efficiency (P.E.), which were about 5 times greater than those of the devices based on DPEPOTPA2 with the shallowest electron trap and the much stronger exciton recombination ability. This work clarified the determinants for the low-triplet-energy hosts and thereby opened the window for the rational molecular design of more complicated and multifunctional host materials.

2. EXPERIMENTAL SECTION

Materials and Instruments. All the reagents and solvents used for synthesis were purchased from Aldrich and Acros companies and used without further purification. 1-(4-Bromophenoxy)-1-2-(diphenylphosphinoyl)-phenoxy-benzene (DPESPOBr), 1-bromo-4-(2,4-dibromo-phenoxy)-5-(diphenylphosphinoyl)-benzene (DPESPOBr3), 4-bromo-2-(diphenylphosphinoyl)-1-2-(diphenylphosphinoyl)-phe-

Scheme 2. Synthetic Procedure of DPE_xPOTPA_n

noxy-benzene (DPEOBr), and 1-bromo-4-(4-bromo-2-(diphenylphosphinoyl)-phenoxy-5-(diphenylphosphinoyl)-benzene (DPEPOBr2) were synthesized according to our previous reports.⁷⁶

¹H NMR spectra were recorded using a Varian Mercury plus 400NB spectrometer relative to tetramethylsilane (TMS) as internal standard. Molecular masses were determined by a FINNIGAN LCQ Electro-Spraying Ionization-Mass Spectrometry (ESI-MS), or a MALDI-TOF-MS. Elemental analyses were performed on a Vario EL III elemental analyzer. Absorption and photoluminescence (PL) emission spectra of the target compound were measured using a SHIMADZU UV-3150 spectrophotometer and a SHIMADZU RF-5301PC spectrophotometer, respectively. Thermogravimetric analysis (TGA) and differential scanning calorimetry (DSC) were performed on Shimadzu DSC-60A and DTG-60A thermal analyzers under nitrogen atmosphere at a heating rate of 10 °C min⁻¹. Cyclic voltammetric (CV) studies were conducted using an Eco Chemie B. V. AUTOLAB potentiostat in a typical three-electrode cell with a platinum sheet working electrode, a platinum wire counter electrode, and a silver/silver nitrate (Ag/Ag⁺) reference electrode. All electrochemical experiments were carried out under a nitrogen atmosphere at room temperature in CH₂Cl₂ for oxidation and THF for reduction. Phosphorescence spectra were measured in dichloromethane using an Edinburgh FPLS 920 fluorescence spectrophotometer at 77 K cooling by liquid nitrogen with a delay of 300 μs using the time-correlated single photon counting (TCSPC) method with a microsecond pulsed Xenon light source for 10 μs to 10 s lifetime measurement, the synchronization photomultiplier for signal collection and the Multi-Channel Scaling Mode of the PCS900 fast counter PC plug-in card for data processing. The thin films of the PO compounds were prepared through vacuum evaporation on glass substrates under the same condition of device fabrication. The morphological characteristics of these films were measured with an atom force microscope (AFM) Agilent 5100 under the tapping mode.

General Procedure of Suzuki Coupling. In Ar₂, 6 equiv. of aq. NaOH (2 M) was added to a stirred solution of 1 equiv. of the bromide, 1.5 equiv. of N,N-diphenyl-4-(4,4,5,5-tetramethyl-1,3,2-dioxaborolan-2-yl)aniline, 0.1 equiv. of Pd(PPh₃)₄ and 0.1 equiv. of TBAB in 10 mL of THF. The reaction mixture was heated to 80 °C and stirred for 24 h. The reaction was quenched by 10 mL of aq. NH₄Cl, and extracted by dichloromethane (3 × 10 mL). The organic layer was dried with anhydride Na₂SO₄. The solvent was removed in vacuo, and then the residue was purified by flash column chromatography.

4'-(2-(Diphenylphosphoryl)phenoxy)-N,N-diphenylbiphenyl-4-amine (DPESPOTPA). DPESPOTPA was purified by flash column chromatography using petroleum ether/ethyl acetate (2:1–0:1) as eluent to afford 307 mg of white powder with the yield of 50%. ¹H NMR (TMS, CDCl₃, 400 MHz): δ = 8.104 (qd, J₁ = 7.6 Hz, J₂ = 12.8 Hz, J₃ = 1.6 Hz, 1H), 7.810 (q, J₁ = 7.0 Hz, J₂ = 12.6 Hz, 4H), 7.542–7.368 (m, 11H), 7.332–7.234 (m, 5H), 7.188–7.098 (m, 6H), 7.056 (t, J = 7.4 Hz, 2H), 6.818 (q, J₁ = 5.2 Hz, J₂ = 8.0 Hz, 1H), 6.659 ppm (d, J = 8.8 Hz, 2H). LDI-TOF: m/z (%): 613 (100) M⁺. Elemental anal. Calcd for C₄₂H₃₂N₂O₂P (%): C, 82.20; H, 5.26; N, 2.28; O, 5.21. Found: C, 82.22; H, 5.25; N, 2.47; O, 5.36.

4'-(4'-(Diphenylamino)biphenyl-4-yloxy)-3'-(diphenylphosphoryl)-N,N-diphenylbiphenyl-4-amine (DPESPOTPA2). DPESPOTPA2 was purified by flash column chromatography using petroleum ether/ethyl acetate (2:1–0:1) as eluent to afford 86 mg of white powder with the yield of 20%. ¹H NMR (TMS, CDCl₃, 400 M Hz): δ = 8.370 (dd, J = 2.4 Hz, 13.6 Hz, 1H); 7.845 (q, J = 7.0 Hz, 12.6 Hz, 4H); 7.672 (dd, J = 2.4 Hz, 8.4 Hz, 1H); 7.541–7.474 (m, 4H); 7.477–7.381 (m, 8H); 7.336–7.258 (m, 8H); 7.196–7.114 (m, 12H); 7.064 (t, J = 7.4 Hz, 4H); 6.877 (q, J = 5.2 Hz, 8.4 Hz, 1H); 6.683 ppm (d, J = 8.4 Hz, 2H). LDI-TOF: m/z (%): 856 (100) M⁺. Elemental anal. Calcd for C₆₀H₄₅N₂O₂P (%): C, 84.09; H, 5.29; N, 3.27; O, 3.73. Found: C, 84.13; H, 5.30; N, 3.85; O, 3.84.

1-Diphenylamino-4-(2,4-di(diphenylamino)-phenoxy)-5-(diphenylphosphinoyl)-benzene (DPESPOTPA3). DPESPOTPA3 was purified by flash column chromatography using petroleum ether/ethyl acetate (2:1–0:1) as eluent to afford 220 mg of white powder with the yield of 40%. ¹H NMR (TMS, CDCl₃, 400 M Hz): δ = 8.374 (dd, J = 2.4 Hz, 13.2 Hz, 1H); 7.766 (q, J = 7.6 Hz, 12.0 Hz, 4H); 7.634 (dd, J = 2.2 Hz, 8.6 Hz, 1H); 7.537 (d, J = 2.4 Hz, 1H); 7.483 (d, J = 8.4 Hz, 2H); 7.434 (d, J = 8.4 Hz, 2H); 6.838–6.781 (m, 2H); 7.369–7.261 (m, 16H); 7.214 (dd, J₁ = 2.4 Hz, J₂ = 8.4 Hz, 1H); 7.677–7.617 (m, 18H); 7.092 (t, J = 7.2 Hz, 2H); 7.060 (t, 7.2 Hz, 4H); 6.947 (d, J = 8.87 Hz, 2H); 6.791 (q, J₁ = 1.2 Hz, J₂ = 8.4 Hz, 1H); 6.307 ppm (d, J = 8.8 Hz, 1H); LDI-TOF: m/z (%): 1099 (100) M⁺; elemental analysis (%) for C₇₈H₅₈N₃O₂P: C 85.14, H 5.31, N 3.82, O 2.91; found: C 85.11, H 5.33, N 3.90, O 3.05.

3'-(Diphenylphosphoryl)-4'-(2-(diphenylphosphoryl)-phenoxy)-N,N-diphenylbiphenyl-4-amine (DPEPOTPA). purified by flash column chromatography using petroleum ether/ethyl acetate (2:1–0:1) as eluent to afford 456 mg of white powder with the yield of 56%. ¹H NMR (TMS, CDCl₃, 400 M Hz): δ = 7.995 (d, J = 13.2 Hz, 1H); 7.819–7.615 (m, 10H); 7.591–7.202 (m, 20H); 7.149–7.073 (m, 6H); 7.066–7.009 (m, 2H); 6.171–6.097 (m, 1H); 6.097–6.006 ppm (m, 1H). LDI-TOF: m/z (%): 813 (100) M⁺. Elemental anal. Calcd for C₅₄H₄₁N₃O₃P₂ (%): C, 79.69; H, 5.08; N, 1.72; O, 5.90. Found: C, 79.72; H, 5.09; N, 1.88; O, 6.04.

4',4'-Oxybis(3'-(diphenylphosphoryl)-N,N-diphenylbiphenyl-4-amine) (DPEPOTPA2). DPEPOTPA2 was purified by flash column chromatography using petroleum ether/ethyl acetate (2:1–0:1) as eluent to afford 529 mg of white powder with the yield of 50%. ¹H NMR (TMS, CDCl₃, 400 M Hz): δ = 7.945 (d, J = 13.2 Hz, 2H); 7.855–7.615 (m, 8H); 7.562–7.315 (m, 14H); 7.318–7.240 (m, 12H); 7.158–7.111 (m, 8H); 7.111–7.081 (m, 4H); 7.079–7.018 (m, 4H); 6.193–6.078 ppm (m, 2H). LDI-TOF: m/z (%): 1056 (100) M⁺. Elemental anal. Calcd for C₇₈H₅₈N₃O₂P (%): C, 81.80; H, 5.15; N, 2.65; O, 4.54. Found: C, 81.79; H, 5.12; N, 2.77; O, 4.61.

DFT Calculations. The DFT simulations were carried out with different parameters for structure optimizations and vibration analyses. The ground states and triplet states of molecules in vacuum were optimized without any assistance of experimental data by the restricted and unrestricted formalism of Beck's three-parameter hybrid exchange functional⁷⁷ and Lee, Yang, and Parr correlation functional⁷⁸ (B3LYP)/6-31G(d), respectively. The fully optimized stationary points were further characterized by harmonic vibrational frequency analysis to ensure that real local minima had been found without

imaginary vibrational frequency. The total energies were also corrected by zero-point energy both for the ground state and triplet state. The spin density distributions were visualized with Gaussview 3.0. All computations were performed using the Gaussian 03 package.⁷⁹

Device Fabrication and Testing. Before loading into a deposition chamber, the ITO substrate was cleaned with detergents and deionized water, dried in an oven at 120 °C for 4 h, and treated with UV-ozone for 20 min. Devices were fabricated by evaporating organic layers at a rate of 0.1–0.3 nm s⁻¹ onto the ITO substrate sequentially at a pressure below 1 × 10⁻⁶ mbar. Onto the TPBI layer, a layer of LiF with 1 nm thickness was deposited at a rate of 0.1 nm s⁻¹ to improve electron injection. Finally, a 100 nm thick layer of Al was deposited at a rate of 0.6 nm s⁻¹ as the cathode. The emission area of the devices was 0.14 cm² as determined by the overlap area of the anode and the cathode. The EL spectra and CIE coordinates were measured using a PR650 spectra colorimeter. The current–density–voltage and brightness–voltage curves of the devices were measured using a Keithley 2400/2000 source meter and a calibrated silicon photodiode. All the experiments and measurements were carried out at room temperature under ambient conditions. For each host, five devices with the same configurations were fabricated to confirm the performance repeatability. The data reported herein were most close to the average results. The average data are shown in Figure S4 in the Supporting Information with the error bars corresponding to the range of the results.

3. RESULTS AND DISCUSSIONS

3.1. Design and Synthesis. The success of CBP in FIrpic-based PHOLEDs is due to its high endothermic energy transfer efficiency and the deep charge and exciton traps on FIrpic formed by the much lower highest occupied molecular orbital (HOMO, -6.2 eV) and the much higher lowest unoccupied molecular orbital (LUMO, -2.5 eV) of CBP. Therefore, it can hardly reflect independent effects of thermal assistant energy transfer (TAET) and charge and exciton capture (CEC). Theoretically, direct charge recombination on phosphors is more efficient than host-dopant energy transfer. This is evidenced by E.Q.E. of 14% from CEC-involved PHOLEDs,⁷⁵ three times higher than TAET afforded E.Q.E.⁶⁹ Adachi et al. recently also report the remarkably improved E.Q.E. of deep-blue PHOLEDs by the direct charge recombination on dopants through dropping the HOMO of the host to form the hole trap with a depth of 0.1 eV.⁸⁰ Nevertheless, the direct evidence about the significance of CEC on EL performance, especially for low-triplet-energy hosts, is still absent because of the simultaneous involvement of both TAET and CEC in conventional devices. Therefore, with the purpose of independently investigating the effects of CEC, the ideal hosts should be designed with the exactly same TAET to FIrpic and the much different charge capture and recombination abilities. In our previous works, the selective adjustment of electrical properties without changing T_1 was successfully realized.^{31,45,59,76} This made this study probable, since the host-dopant triplet energy gap is one of the key determinants for TAET. Different from our previous works about PO hosts, in which PO moieties mainly served as the electroactive insulating groups to achieve high T_1 and polarize molecules, herein, with no regards to the achievement of high T_1 by PO groups, the insulating feature of PO moieties was utilized to suppress the influence of structural variations on T_1 with the assistance of the meta linkage and ether bridge. TPA was involved to enhance hole transporting ability and achieve the relative low T_1 through forming diphenylbiphenylamine segment. The ratio of TPA and electron transporting DPPO was gradually changed to purposefully adjust molecular electrical properties. The

function of PO moieties in $\text{DPE}_x\text{POTPA}_n$ was tuning their electroactivity without changing T_1 energy levels, which accordingly established the platform to confirm the effects of CEC on the device performance.

$\text{DPE}_x\text{POTPA}_n$ were conveniently prepared from the bromide precursors $\text{DPE}_x\text{POBr}_n$ through Suzuki coupling with *N,N*-diphenyl-4-(4,4,5,5-tetramethyl-1,3,2-dioxaborolan-2-yl)-aniline with moderate yields around 50% (Scheme 2). The structure characterization was established on the basis of mass spectrometry, NMR spectroscopy and elemental analysis.

3.2. Optical Properties. As mentioned above, the similar optical properties of these hosts are the basis for rationally investigating the effect of CEC on the EL performance. Therefore, the UV/vis absorption and photoluminescent (PL) spectra of $\text{DPE}_x\text{POTPA}_n$ in CH_2Cl_2 (× 10⁻⁶ mol L⁻¹) were measured to confirm the selective adjustment of excited state energy by structural variation (Figure 1 and Table 1).

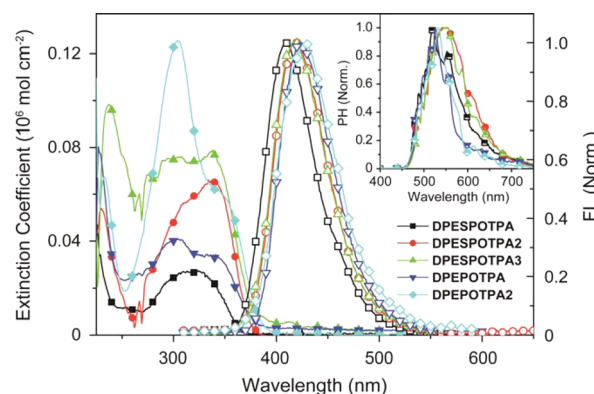


Figure 1. Absorption and emission spectra of $\text{DPE}_x\text{POTPA}_n$ in CH_2Cl_2 (× 10⁻⁶ mol L⁻¹). The phosphorescence (PH) spectra were recorded at 77 K with a delay of 300 μs.

$\text{DPE}_x\text{POTPA}_n$ have three main absorption bands around 320–350, 250–300 and 230 nm, corresponding to $n-\pi^*$ transitions from TPA to diphenylether, $n-\pi^*$ transitions from TPA to DPPO and $\pi-\pi^*$ transitions between TPA and diphenylether. It is showed that the extinction coefficients are exactly in accord with the number of corresponding functional groups, which indicated the strong sensitization ability and antenna effect of TPA and DPPO. PL quantum yields (PLQY) of $\text{DPE}_x\text{POTPA}_n$ were directly proportional to TPA number and in reverse proportion to DPPO number, ascribed to strong electron-donating effect of TPA as chromophore and electron-withdrawing effect of DPPO, respectively (Table 1). Accordingly, the probabilities of radiative transition for the mono-DPPO derivatives are rather high under irradiative excitation, exhibiting their greater potential as electrofluorophores in OLEDs with efficient charge recombination. Estimated from the absorption edges, the first singlet excited energy levels (S_1) of $\text{DPE}_x\text{POTPA}_n$ are gradually reduced due to the conjugation extension with more TPA and/or DPPO groups (Table 1). It is showed that one additional TPA and DPPO can result in the S_1 reductions of ~0.1 and 0.15 eV, respectively. Because S_1 is approximately equivalent with the HOMO–LUMO energy gap, obviously, through adjusting the functional group ratios, the FMO energy levels of the hosts can be purposefully tuned to fit with those of the adjacent CTLs for improving carrier injection and transportation and form the charge traps with suitable depths. In solid state, absorption and PL spectra of

Table 1. Physical Properties of DPE_xPOTPA_n

compd	absorption (nm)	emission ^c (nm)	PLQY ^d (%)	S ₁ (eV)	T ₁ (eV)	T _g /T _m /T ^d (°C)	RMS (nm)	HOMO (eV)	LUMO (eV)
DPESPOTPA	324, 255, 226 ^a	408(54) ^a	90	3.38 ^e	2.63 ^g	-/ 119/416	1.14	-5.91 ^h	-2.44 ^h / -2.53 ⁱ -0.93 ^f
	336, 262, 225 ^b	407(50) ^b		4.08 ^f	2.65 ^f			-5.01 ^f	
DPESPOTPA2	339, 308, 231 ^a	416(58) ^a	98	3.26 ^e	2.63 ^g	123/-/ 492	1.19	-5.91 ^h	-2.62 ^h / -2.65 ⁱ -0.98 ^f
	345, 222 ^b	414(53) ^b		3.86 ^f	2.63 ^f			-4.84 ^f	
DPESPOTPA3	337, 300, 274, 238 ^a	416(59) ^a	100	3.16 ^e	2.63 ^g	146/-/ 509	1.50	-5.75 ^h	-2.56 ^h / -2.59 ⁱ -1.06 ^f
	343, 305, 233 ^b	413(48) ^b		3.78 ^f	2.69 ^f			-4.84 ^f	
DPEPOTPA	342,304,227 ^a	422(59) ^a	40	3.22 ^e	2.63 ^g	-/239/393	0.41	-5.90 ^h	-2.63 ^h / -2.68 ⁱ -0.87 ^f
	343, 264, 221 ^b	422(58) ^b		4.03 ^f	2.67 ^f			-4.90 ^f	
DPEPOTPA2	345, 304, 233 ^a	428(65) ^a	48	3.11 ^e	2.63 ^g	206/254/466	0.75	-5.88 ^h	-2.70 ^h / -2.77 ⁱ -0.92 ^f
	343, 302, 230 ^b	467(142) ^b		3.95 ^f	2.65 ^f			-4.87 ^f	

^aIn CH₂Cl₂ (× 10⁻⁶ mol L⁻¹). ^bIn film. ^cfwhm was in parentheses. ^dCalculated by using 9,10-diphenylanthracene as standard. ^eEstimated according to the absorption edges. ^fDFT calculated results. ^gCalculated according to the 0-0 transitions of the phosphorescence spectra. ^hCalculated according to the equation $E_{\text{HOMO/LUMO}} = 4.78 + \text{onset voltage}$. ⁱEstimated according to the optical energy gaps and the experimental HOMOs.

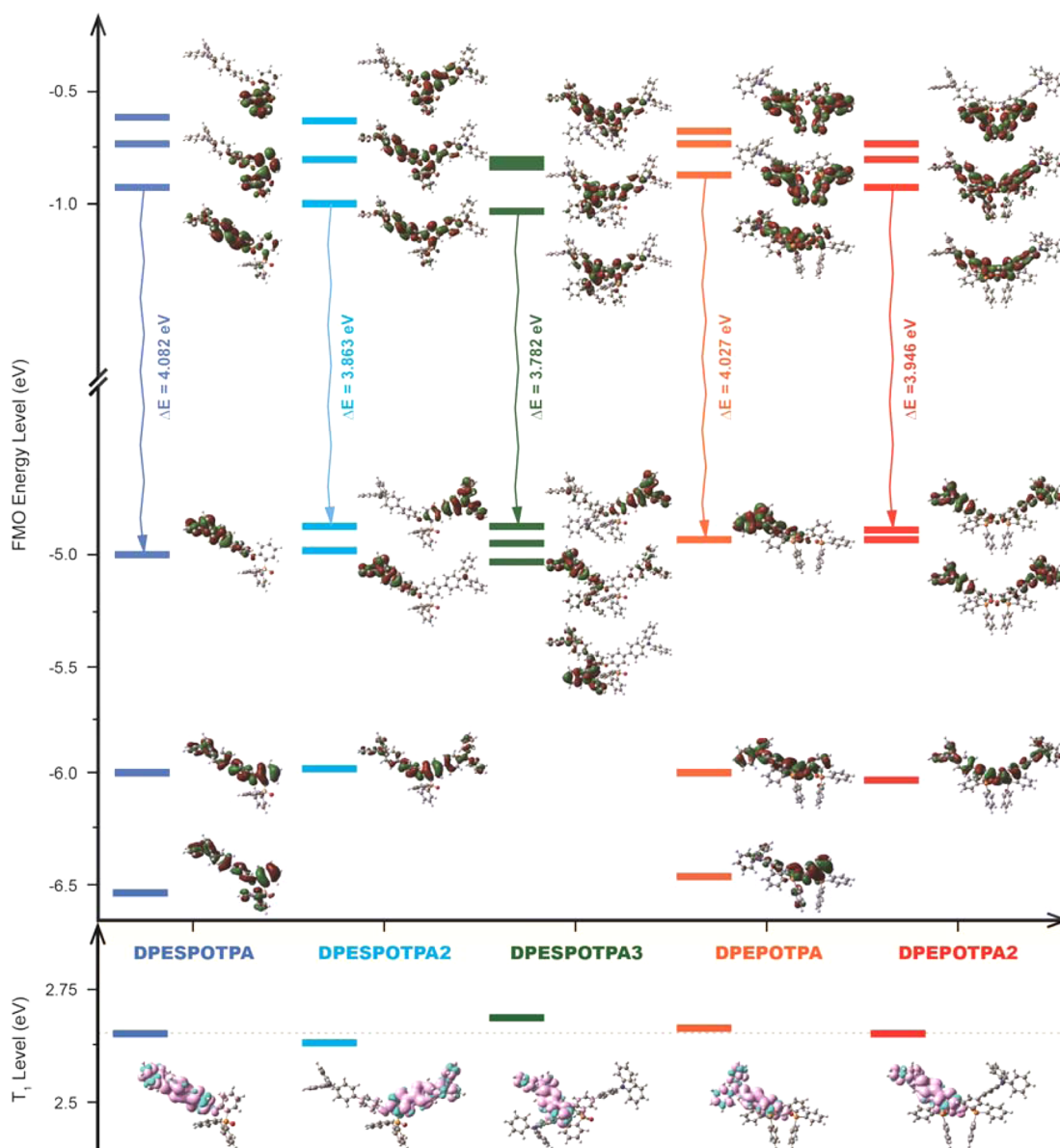


Figure 2. Contours of FMOs for DPE_xPOTPA_n, and the spin density distributions of their T₁ values by DFT calculation.

DPE_xPOTPA_n were almost the same as those in dilute solution with the preserved fine structures and the similar absorption

band wavelengths, which indicated the suppressed aggregation and restrained intermolecular interactions, except for DPE-

POTPA2, whose symmetrical structure resulted in the aggregation-induced bathochromic shifts (Table 1).

T_1 of these molecules was much concerned because of its direct relevancy to triplet energy transfer process, which was estimated from the 0–0 transitions in their time-resolved low-temperature phosphorescent (PH) spectra (inset in Figure 1). As demonstrated in our previous works about mixed linkage strategy, the combined meta and multi-insulating linkage endows $\text{DPE}_x\text{POTPA}_n$ with the almost same PH spectra in shape and peak wavelength, resulting in their same T_1 of 2.63 eV. Low-triplet energy diphenylbiphenylamine segments as chromophore in these molecules should make the main contributions to their T_1 excited state, which was further evidenced by the same spin density distributions (SDD) on TPA and partial diphenylether according to density function theory (DFT) calculation (Figure 2 below),^{81,82} whereas insulating linkages almost have no contributions to T_1 state. Therefore, in the systems like $\text{DPE}_x\text{POTPA}_n$, T_1 states can be feasibly controlled at the same time of adjusting the molecular structure and functional group ratio for tuning electrical properties. The slight lower T_1 of $\text{DPE}_x\text{POTPA}_n$ than 2.65 eV of Flrpic gives rise to the similar TAET processes.

According to optical analysis, through varying the number and ratio of the functional groups, much different S_1 and the radiative transition characteristics of $\text{DPE}_x\text{POTPA}_n$ were successfully realized to establish the different charge traps and charge recombination possibilities in PHOLEDs, which provides a flexible platform for rationally investigating the effect of CEC on device performance.

3.3. Electrical Properties. The competition on charge capture between the hosts and dopants in EMLs is mainly determined by the differences of their FMO energy levels. Therefore, we first performed the structural DFT optimization of the ground-state $\text{DPE}_x\text{POTPA}_n$ in vacuum (Figure 2 above). It is showed that electron cloud densities of their HOMOs are mainly localized on the electron-donating groups, especially TPA.^{52,82} Furthermore, DPPOs are almost not involved in the frontier OMOs. Contrarily, although the LUMOs are also mainly localized on TPA and diphenylether groups because of their bigger conjugation, DPPOs make considerable contributions to the frontier unoccupied molecular orbitals (UMOs). Especially for DPEPOTPA_n , their LUMO+1 and/or LUMO+2 are mainly localized on DPPO groups. Therefore, the incorporation of DPPO moieties can facilitate the electron injection and transportation.⁸¹ Furthermore, because of the strong electron-donating ability of TPA, the incorporation of one more DPPO in DPEPOTPA_n does not dramatically weaken their hole injecting/transporting ability. Although conjugation, molecular configuration and number and ratio of functional groups are three main determinants for FMO energy levels of these molecules, number and ratio of functional groups is predominant because the former two are also actually related to it.

The experimental HOMO and LUMO energy levels were estimated with cyclic voltammetrical (CV) analysis (Figure 3a). According to the oxidation curves of DPEPOTPA_n , all of the compounds exhibited one reversible oxidation peak at ~ 1.35 V and two irreversible oxidation peaks at ~ 1.75 and 2.0 V, which can be ascribed to TPA, diphenylether and DPPO, respectively. Except for DPESPOTPA3 , the onset voltages of other four compounds are very similar as around 1.1 V, corresponding to the HOMO energy levels about -5.9 eV (Table 1). The highest proportion of TPA moieties in DPESPOTPA3 results

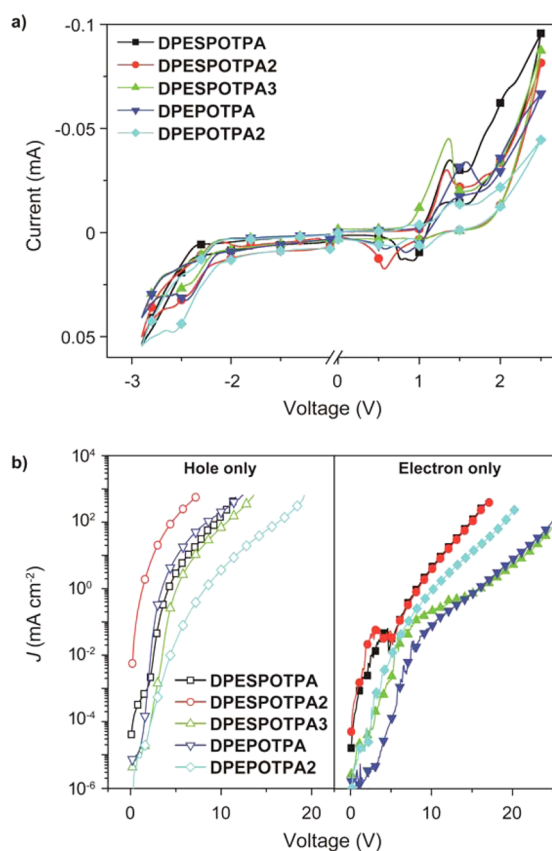


Figure 3. (a) Cyclic voltammograms of $\text{DPE}_x\text{POTPA}_n$ measured in CH_2Cl_2 for oxidation and THF for reduction at room temperature with the scanning rate of 100 mV S^{-1} and tetra-*n*-butylammonium hexafluorophosphate as supporting electrolyte (0.1 mol L^{-1}); (b) IV characteristics of nominal single-carrier transporting devices based on $\text{DPE}_x\text{POTPA}_n$.

in much smaller onset voltage at ~ 0.95 V, corresponding to the HOMO of approximately -5.75 eV. Taking account of the HOMO of Flrpic as -5.6 eV, the depth of the hole trap formed between DPESPOTPA3 and Flrpic is only 0.15 eV, much shallower than ~ 0.3 eV for the other hosts. As shown in Scheme 1, the efficient charge capture requires the trap depth at least 0.2 eV to overcome the disturbance from thermal fluctuations. Therefore, when doped in the matrixes of $\text{DPE}_x\text{POTPA}_n$ ($n = 1$ and 2), Flrpic can efficiently trap the hole injected from cathode, whereas for the DPESPOTPA3 -Flrpic doping system, isotropic hole migration is possible with the heat assistance. It is indicated that the LUMO energy levels of $\text{DPE}_x\text{POTPA}_n$ are dependent on the functional groups number and ratio and the molecular conjugation degree (Table 1). Accordingly, DPEPOTPA2 with two DPPO groups and symmetrical configuration achieves the deepest LUMO energy levels of -2.70 eV, which is about 0.05 eV lower than those of DPEPOTPA and DPESPOTPA2 , and about 0.15 and 0.25 eV lower than those of DPESPOTPA3 and DPESPOTPA , respectively. Thus, the electron trap formed between Flrpic and $\text{DPE}_x\text{POTPA}_n$ ($n = 1$ and 2) is too shallow with a depth of only 0.1–0.15 eV to hardly confine electron on the dopants. However, when doped in DPESPOTPA and DPESPOTPA3 , Flrpic can realize the efficient electron capture with a suitable electron trap depth of about 0.2–0.4 eV. Therefore, in these hosts, DPESPOTPA can endow Flrpic with the strongest capability for both hole and electron capture, while in

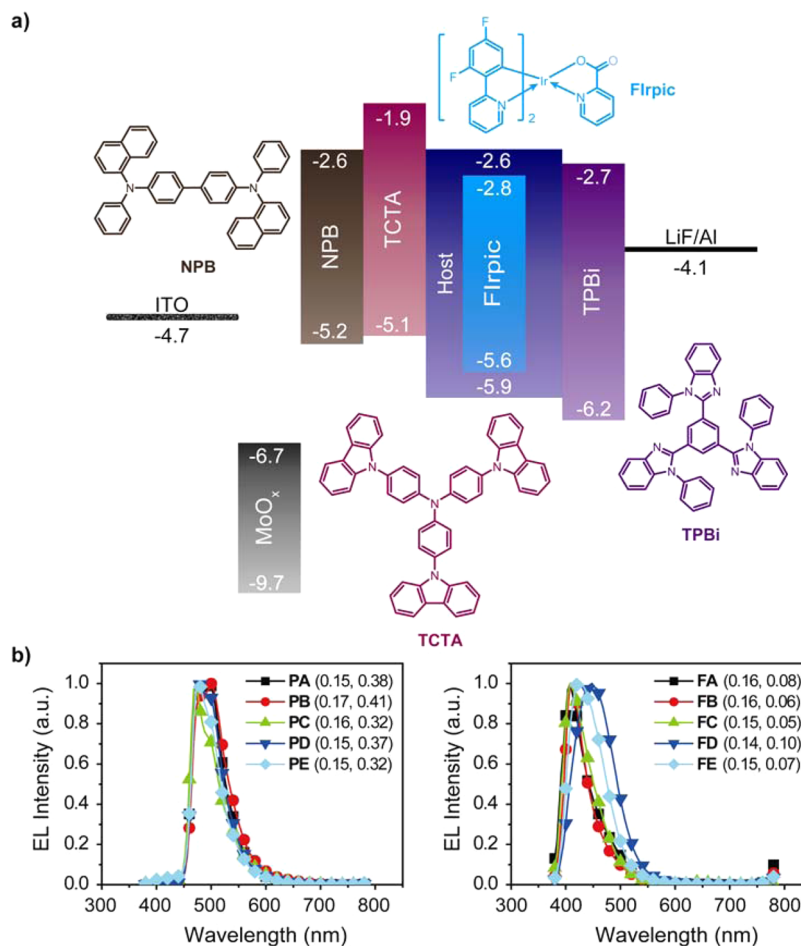


Figure 4. (a) Energy level scheme of the PHOLEDs; (b) EL spectra of phosphorescent (left) and fluorescent (right) devices with the corresponding CIE coordinates.

DPEPOTPA2 and DPESPOTPA3, the electron and hole capture ability of Flrpic is the weakest, respectively.

The carrier transporting ability of DPE_xPOTPA_n was further assessed with the IV characteristics of their nominal single-carrier transporting devices with the structures of ITO|MoO₃ (8 nm)|NPB (20 nm)|Host (40 nm)|NPB (30 nm)|MoO₃ (8 nm)|Al for hole-only and ITO|LiF (1 nm)|TPBi (30 nm)|Host (40 nm)|TPBi (20 nm)|LiF (1 nm)|Al for electron-only, respectively, in which MoO₃ and LiF served as hole- and electron-injecting layers, NPB is N,N-bis(naphthylphenyl)-4,4'-biphenyldiamine as the hole-transporting layer (HTL), TPBi is 1,3,5-tris(1-phenyl-1H-benzodimidazol-2-yl)benzene as electron-transporting hole-blocking layer, respectively (Figure 3b). NPB and TPBi were involved to modify the interfaces and simulate the environment in emitting devices. Thicknesses of hole-only and electron-only devices were the same to make comparison between them rational. The hole-only current density (*J*) of DPESPOTPA2 and DPEPOTPA2 were the highest and lowest among these derivatives, respectively, while those of other materials were similar. The electron-only *J* of DPESPOTPA was also almost the biggest, comparable with that of DPESPOTPA. It is noticed that the electron-only *J* of DPESPOTPA3 and DPEPOTPA were very approximate, which were lower than that of DPEPOTPA2. It indicated that the carrier transporting properties were the integrated results of molecular compositions and intermolecular inter-

actions. Furthermore, these ternary hybrids showed the uniform feature of hole-dominant volt-ampere characteristics.

The exciton stability directly determines the luminescent performance of the phosphors in the devices, so it is desired if electron and hole were both localized on Flrpic to form the most stable Frenkel excitons like the situation of DPESPOTPA. However, DPESPOTPA2 and DPEPOTPA_n (*n* = 1 and 2) and DPESPOTPA3 can only efficiently confine the hole or electron on Flrpic, respectively, to afford the formation of Wannier–Mott excitons with the weaker stability. Because the electron would be the minority carrier in the devices of these hole-transporting predominant hosts, the weaker capture ability for electron is more inferior to the number and stability of excitons. In this sense, DPEPOTPA2 might be the worst host for Flrpic among these materials.

3.4. EL Performance of DPE_xPOTPA_n and the Influence of Charge and Exciton Capture. It can be confirmed that DPE_xPOTPA_n provide a platform to selectively investigate CEC effect on the basis of the probably same energy transfer process and the much different electrical properties. Accordingly, their Flrpic-based PHOLEDs with the configuration of ITO|MoO₃ (8 nm)|NPB (70 nm)|TCTA (5 nm)|Host: 15% Flrpic (20 nm)|TPBi (30 nm)|LiF (1 nm)|Al were fabricated as PA-PE, corresponding to DPESPOTPA_n (*n* = 1, 2 and 3) and DPEPOTPA_n (*n* = 1 and 2), respectively, where TCTA is tris(4-(9H-carbazol-9-yl)phenyl)amine as exciton-blocking layer (Figure 4a). It is showed that since the HOMO and

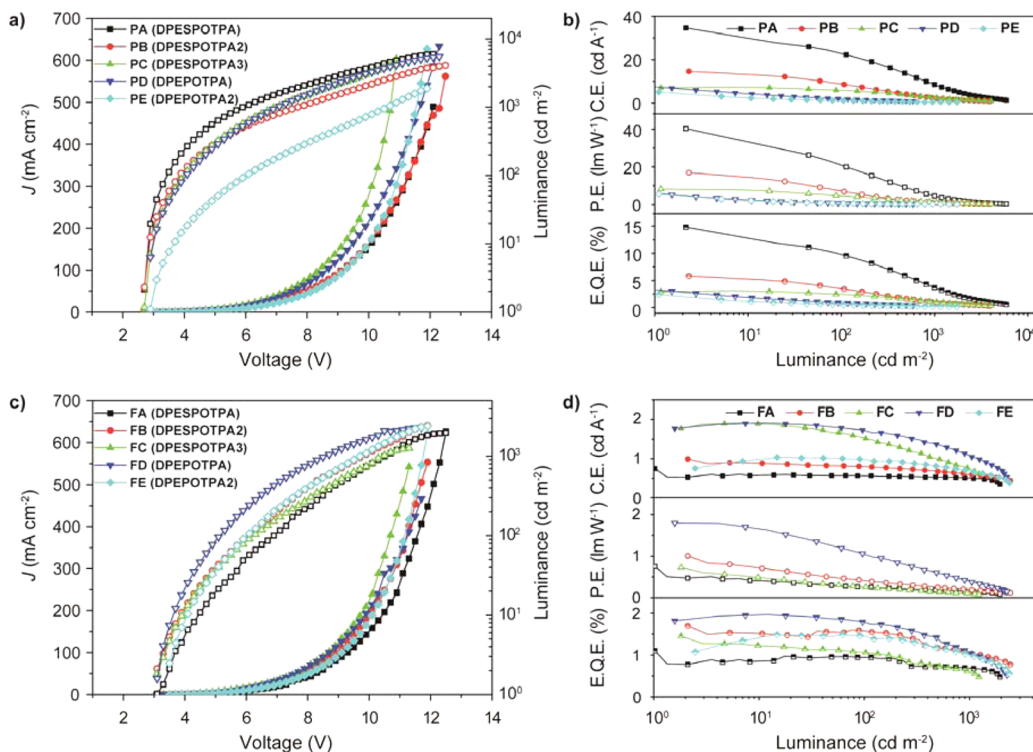


Figure 5. Brightness–current density (J)–voltage curves and efficiency curves of (a, b) phosphorescent PA-PE and (c, d) fluorescent FA-FE based on $\text{DPE}_x\text{POTPA}_n$.

LUMO of Flrpic are shallower and deeper than those of $\text{DPE}_x\text{POTPA}_n$, the hole and electron traps can be formed on Flrpic with the different depths. The similar energy transfer process from hosts to Flrpic was further evidenced by EL emissions definitely from Flrpic without any host emissions observed (Figure 4b). Therefore, it can be expected to figure out CEC effect in the low-triplet-energy-host-involved electrophosphorescence process according to EL performance of PA-PE.

Operating voltages of these devices were rather low that the onset voltages for all of the PHOLEDs were lower than 3 V (Figure 5a). PA showed the lowest driving voltages as 2.7 V for onset, <3.5 V at 100 cd m^{-2} and <6.1 V at 1000 cd m^{-2} , respectively. The latter two were about 0.4 and 1.6 V lower than those of PB. PC and PD had the equal driving voltages for onset, 100 and 1000 cd m^{-2} , which were 0.2, 2.0, and 3.6 V lower than those of PE. Taking account of the difference less than 1.0 eV between the work functions of electrodes, it is believed that the reduction of S_1 is beneficial to the balanced carrier injection. As mentioned above, through the conjugation extension by tuning the functional group number and ratio, S_1 of $\text{DPE}_x\text{POTPA}_n$ was gradually reduced without changing their T_1 , in which S_1 of DPESPOTPA is the highest and that of DPEPOTPA2 is the lowest. However, the tendency of the device operating voltages was just inverted that the driving voltage seemed to be inversely proportional to S_1 of the hosts (Table 2), which was also inconsistent with the results of CV analysis and IV characteristics of the single-carrier transporting devices. Actually, since the driving voltage is defined regarding to the specific brightness, luminescent performance of the device should be one of the determinants for operating voltage, which reflects the utilization of injected carriers and the confinement efficiency of exciton on phosphors. This was further testified by much increased differences between the

Table 2. EL Performance of $\text{DPE}_x\text{POTPA}_n$

device	operating voltage (V) ^a	maximum brightness (cd m^{-2}) ^b	C.E. (cd A^{-1}) ^c	P.E. (lm W^{-1}) ^c	E.Q.E. (%) ^c
PA	2.7, <3.5, <6.1	5979 (12.1, 489)	34.6, 22.3	40.3, 20.0	14.8, 9.5
PB	2.7, <3.9, <7.7	4090 (12.5, 562)	14.6, 8.6	16.9, 6.9	5.8, 3.4
PC	2.7, <4.1, <7.1	4242 (10.9, 604)	7.3, 5.7	8.2, 4.4	3.1, 2.4
PD	2.7, <4.1, <7.1	5500 (12.3, 633)	7.4, 1.9	5.9, 0.7	3.2, 0.8
PE	2.9, <6.1, <10.7	1877 (11.9, 627)	5.1, 1.1	5.5, 0.5	2.4, 0.5
FA	3.1, <6.9, <10.7	1976 (12.5, 626)	0.75, 0.56	0.76, 0.26	1.10, 0.95
FB	3.1, <6.1, <9.9	2444 (11.9, 554)	1.00, 0.79	1.01, 0.41	1.70, 1.56
FC	3.1, <6.3, <10.5	1253 (11.3, 542)	1.92, 1.51	0.73, 0.25	1.45, 1.06
FD	3.1, <5.3, <8.7	2283 (11.7, 466)	1.92, 1.97	1.79, 0.99	1.97, 1.73
FE	3.5, <6.1, <9.7	2389 (11.9, 621)	1.03, 0.97	0.75, 0.50	1.48, 1.43

^aIn the order of onset, 100 and 1000 cd m^{-2} . ^bThe corresponding voltage (V) and J (mA cm^{-2}) were listed in the parentheses. ^cIn the order of maximum and 100 cd m^{-2} .

driving voltages of PA-PE at higher brightness, which should be ascribed to the more stringent demand for efficient utilization of carriers and exciton at higher concentrations.

EL efficiencies of PA-PE showed more direct information about the relationship between the host properties and the utilization efficiency of carriers and exciton (Figure 5a and Table 2). It is showed that DPESPOTPA endowed PA with the highest maximum efficiencies among these PHOLEDs as

34.6 cd A⁻¹ for current efficiency (C.E.), 40.3 lm W⁻¹ for P.E. and 14.8% for E.Q.E., which were favorable among the most efficient FIrpic-based PHOLEDs and comparable to the devices involving high-triplet-energy host materials. At the practical luminance of 100 cd m⁻², its efficiencies remained as 22.3 cd A⁻¹, 20.0 lm W⁻¹, and 9.5%, indicating the suppressed quenching processes at the high carrier and exciton concentrations. However, the maximum efficiencies of **PB** were sharply reduced to be less than an half of those of **PA**, which were further decreased at 100 cd m⁻² with a bigger roll-off more than 40% for E.Q.E. The involvement of **DPESPOTPA3** and **DPEPOTPA** in **PC** and **PD** resulted in their efficiency losses for about 50% compared with **PB**. The difference between **PC** and **PD** was that the efficiencies of the former was much more stable than those of the latter, which should be ascribed to the more stable FIrpic-localized excitons in **DPESPOTPA3** matrix. Finally, **PE**, using **DPEPOTPA2** as host, revealed the lowest efficiencies and the most serious efficiency roll-offs. Because T_1 values of **DPEPOTPA_n** are equivalent to afford the similar host-dopant energy transfer process, the striking difference between EL performances of these DPPO-TPA hybrids should be mainly ascribed to their various electrical properties, especially the capture ability of carriers and exciton.

It is believed that the direct exciton recombination on dopant is more efficient than the typical two-step EL process involving exciton recombination on host and sequential host-dopant energy transfer, which is more reasonable for low-triplet-energy hosts because of inefficient host-to-dopant energy transfer. In this sense, the exciton capture by low-triplet-energy hosts is inferior in achieving high EL efficiencies. Taking account of the direct proportionality between exciton capture ability and exciton recombination efficiency, we fabricated OLEDs using **DPEPOTPA_n** as EMLs (20 nm) with the same configurations as their PHOLEDs, corresponding to **FA-FE**, to evaluate exciton recombination efficiencies of these host materials. It is showed that all of the fluorescent OLEDs gave out deep-blue lights similar to the solid-state PL emissions of the corresponding DPPO-TPA hybrids (Figure 4c). Since hole is the majority carrier in these devices, **DPEPOTPA2** with the weakest hole-transporting ability still resulted in the highest onset voltage of **FE** (Figure 5c and Table 2). However, at 100 and 1000 cd m⁻², its driving voltages were 0.8 and 1.0 V lower than those of **FA** based on **DPESPOTPA**. The driving voltages of **FB** and **FC** were close to those of **FE**, while **DPEPOTPA** supported **FD** with the lowest operating voltages, which were 0.8 and 1.0 V lower than those of **FE**. More importantly, **FD** achieved the highest maximum efficiencies among these devices as 1.92 cd A⁻¹, 1.79 lm W⁻¹, and 1.97%, accompanied with the well-controlled roll-off as 12% for E.Q.E. at 100 cd m⁻², which were comparable with the reported best results about the nondoped deep-blue fluorescent OLEDs (Figure 5d and Table 2). Contrarily, the maximum efficiencies of **FA** became the lowest as only 0.75 cd A⁻¹, 0.76 lm W⁻¹ and 1.10%, which implied the remarkably weaker exciton recombination ability of **DPESPOTPA**. On the basis of E.Q.E., the exciton recombination efficiency (γ) can be derived as

$$\gamma = \frac{\Phi_{\text{EL}}}{\Phi_{\text{PL}}\chi\eta_{\text{OC}}} \quad (1)$$

Where Φ_{EL} is E.Q.E., Φ_{PL} is PLQY, η_{oc} is outcoupling factor as 0.25 for organic solid, and χ is the fraction of excitons as 0.4 for

conjugated fluophors. γ is equal to 1 when the injected carriers were completely recombined. γ of **FA-FE** are calculated according to their maximum E.Q.E. as 0.11, 0.17, 0.15, 0.49, and 0.31, respectively. Therefore, the exciton recombination ability of **DPESPOTPA** is the weakest among these materials, whereas **DPEPOTPA_n** are much stronger in this aspect compared with their mono-DPPO analogues.

As a summary, the orders of the HOMO, LUMO energy levels and exciton recombination abilities for these hosts were **DPESPOTPA** = **DPESPOTPA2** < **DPEPOTPA** < **DPEPOTPA2** < **DPESPOTPA3**, **DPEPOTPA2** < **DPEPOTPA** < **DPESPOTPA2** < **DPESPOTPA3** < **DPESPOTPA** and **DPESPOTPA** < **DPESPOTPA3** < **DPESPOTPA2** < **DPEPOTPA2** < **DPEPOTPA**, respectively. The relationship between the carrier and exciton capture ability of the hosts and their EL performance was illustrated in Figure 6 by establishing

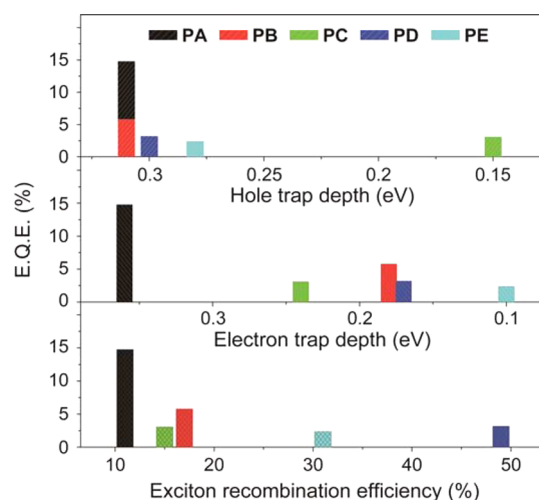


Figure 6. Correlation between the charge trap depths in **PA-PE** and the exciton recombination efficiencies of **DPEPOTPA_n** and the maximum E.Q.E. of the corresponding PHOLEDs.

the correspondence between E.Q.E. and the carrier trap depths on FIrpic and γ of the hosts. It was convincible that the highest efficiencies of **PA** were the combined results of the deepest hole and electron traps on FIrpic and the weakest exciton recombination ability of **DPESPOTPA**, which gave rise to the thoroughly direct carrier and exciton capture by FIrpic so as to avoid the efficiency loss through irreversible energy transfer to nonradiative T_1 of **DPESPOTPA**. For **PB**, where the hole trap depth on FIrpic was equivalent to that for **PA**, the higher γ of **DPESPOTPA2** and the remarkable reduced electron trap depth made the efficiencies declined sharply, in which the shallow electron trap (<0.2 eV) on FIrpic in **PB** should be the main reason because of the unstable electron capture. The depth of the hole trap formed between FIrpic and **DPESPOTPA3** was the smallest as 0.15 eV, accompanied with the electron trap of just 0.24 eV. Therefore, although γ of **DPESPOTPA3** was only 0.15, the inefficient hole and electron capture by FIrpic still led to the further efficiency reduction of **PC**. The exciton recombination abilities of **DPEPOTPA_n** were significantly enhanced, especially for **DPEPOTPA** with γ about 0.5; meanwhile the electron traps between them and FIrpic are only 0.17 and 0.1 eV, even if the hole traps are deep enough to confine the hole on FIrpic. Therefore, **PD** and **PE** revealed the much lower efficiencies compared with other

PHOLEDs. It is noticeable that the carrier capture seems more dominant than exciton capture because the latter actually is dependent on the former. Furthermore, because electron is minority carrier, the electron capture ability becomes more important to determine the final exciton location, which is consistent with the higher efficiencies of PD based on DPEPOTPA with the highest γ than those of PE based on DPEPOTPA2 with the shallowest electron trap.

Therefore, the effective confinement of carrier and exciton on phosphorescent dopants is the most important determinant for low-triplet-energy host involved PHOLEDs. Because the low-energy-gap hosts are theoretically advantageous in reducing operating voltages, the achievement of high efficiencies makes this kind of host materials promising in portable applications.

4. CONCLUSIONS

A series of DPPO-TPA hybrids, namely DPE_xPOTPA_n, were prepared and utilized to take insight into the determinants of low-triplet-energy hosts for efficient PHOLEDs. The influence of CEC effect on EL performance was independently investigated on the basis of their similar irreversible energy transfer processes conjectured by their same T_1 of 2.63 eV. Through tuning FMO energy levels by varying functional group number and ratio, the depths of the carrier traps formed between these hosts and FIrpic are gradually adjusted from 0.15 to 0.31 eV and 0.03 to 0.27 eV for hole and electron, respectively. The exciton recombination abilities of the hosts were further evaluated with γ of their fluorescent OLEDs, which indicated the superiority of DPEPOTPA_n in exciton capture than DPESPOTPA_n. According to the correspondence between E.Q.E. of the FIrpic-based PHOLEDs and the carrier trap depth and γ of the hosts, it is obvious that the direct and efficient carrier and exciton capture by FIrpic is beneficial to improve efficiencies and reduce efficiency roll-offs. As a result, DPESPOTPA with the deepest hole and electron traps and the weakest exciton capture ability endowed its FIrpic-based PHOLED with the best EL performance including the maximum efficiencies about 35 cd A⁻¹, 40 lm W⁻¹ and 15%, which were favorable among the best results about FIrpic-based devices. Therefore, it is clarified that with the effective confinement of carrier and exciton, especially the minority carrier, on phosphorescent dopants, it is feasible to achieve high efficiencies through low-triplet-energy hosts. Because carrier capture can be readily tuned through modulating FMO energy levels of hosts to form carrier traps on dopants, this work actually established the specific design rule for low-triplet-energy hosts and revealed their great advantages in low-driving-voltage applications.

■ ASSOCIATED CONTENT

Supporting Information

Morphological and thermal properties of the films, current density–efficiency curves of the devices and device repeatability data. This material is available free of charge via the Internet at <http://pubs.acs.org>.

■ AUTHOR INFORMATION

Corresponding Authors

*E-mail: hxu@hlju.edu.cn.

*E-mail: mdg1014@ciac.jl.cn.

Author Contributions

[†]Authors C.H. and F.Z. contributed equally.

Notes

The authors declare no competing financial interest.

■ ACKNOWLEDGMENTS

This project was financially supported by NSFC (50903028, 61176020 and 51373050), New Century Excellent Talents Supporting Program of MOE (NCET-12-0706), Program for Innovative Research Team in University (MOE) (IRT-1237), New Key Project of MOE (212039), New Century Excellent Talents Developing Program of Heilongjiang Province (1252-NCET-005), Education Bureau of Heilongjiang Province (10td03), and the Supporting Program of High-Level Talents of HLJU (2010hdt08).

■ REFERENCES

- (1) Shen, Z.; Burrows, P. E.; Bulovic, V.; Forrest, S. R.; Thompson, M. E. *Science* **1997**, *276*, 2009.
- (2) Muller, C. D.; Falcou, A.; Reckefuss, N.; Rojahn, M.; Wiederhirn, V.; Rudati, P.; Frohne, H.; Nuyken, O.; Becker, H.; Meerholz, K. *Nature* **2003**, *421*, 829.
- (3) Burn, P. L.; Lo, S. C.; Samuel, I. D. W. *Adv. Mater.* **2007**, *19*, 1675.
- (4) Tao, Y.; Yang, C.; Qin, J. *Chem. Soc. Rev.* **2011**, *40*, 2943.
- (5) Zhu, X.-H.; Peng, J.; Cao, Y.; Roncali, J. *Chem. Soc. Rev.* **2011**, *40*, 3509.
- (6) Hong, Y.; Lam, J. W. Y.; Tang, B. Z. *Chem. Soc. Rev.* **2011**, *40*, 5361.
- (7) Huang, W.; Mi, B.; Gao, Z. *Organic Electronics*, 1st ed.; Science Press: Beijing, 2011.
- (8) Wu, H.; Ying, L.; Yang, W.; Cao, Y. *Chem. Soc. Rev.* **2009**, *38*, 3391.
- (9) Reineke, S.; Lindner, F.; Schwartz, G.; Seidler, N.; Walzer, K.; Lussem, B.; Leo, K. *Nature* **2009**, *459*, 234.
- (10) Jou, J.-H.; Hsieh, C.-Y.; Tseng, J.-R.; Peng, S.-H.; Jou, Y.-C.; Hong, J. H.; Shen, S.-M.; Tang, M.-C.; Chen, P.-C.; Lin, C.-H. *Adv. Funct. Mater.* **2013**, *23*, 2750.
- (11) Zhu, M.; Yang, C. *Chem. Soc. Rev.* **2013**, *42*, 4963.
- (12) Su, S. J.; Takahashi, Y.; Chiba, T.; Takeda, T.; Kido, J. *Adv. Funct. Mater.* **2009**, *19*, 1260.
- (13) Lee, J.; Chopra, N.; Eom, S.-H.; Zheng, Y.; Xue, J.; So, F. *Proc. SPIE* **2008**, 70511T.
- (14) Tokito, S.; Iijima, T.; Suzuri, Y.; Kita, H.; Tsuzuki, T.; Sato, F. *Appl. Phys. Lett.* **2003**, *83*, 569.
- (15) Trattig, R.; Pevzner, L.; Jäger, M.; Schlesinger, R.; Nardi, M. V.; Ligorio, G.; Christodoulou, C.; Koch, N.; Baumgarten, M.; Müllen, K.; List, E. J. W. *Adv. Funct. Mater.* **2013**, *23*, 4897.
- (16) Duan, L.; Zhang, D.; Wu, K.; Huang, X.; Wang, L.; Qiu, Y. *Adv. Funct. Mater.* **2011**, *21*, 3540.
- (17) Sasabe, H.; Gonmori, E.; Chiba, T.; Li, Y. J.; Tanaka, D.; Su, S. J.; Takeda, T.; Pu, Y. J.; Nakayama, K. I.; Kido, J. *Chem. Mater.* **2008**, *20*, 5951.
- (18) Ye, S. H.; Liu, Y. Q.; Di, C. A.; Xi, H. X.; Wu, W. P.; Wen, Y. G.; Lu, K.; Du, C. Y.; Liu, Y.; Yu, G. *Chem. Mater.* **2009**, *21*, 1333.
- (19) Matsushima, T.; Adachi, C. *Chem. Mater.* **2008**, *20*, 2881.
- (20) Xiao, L.; Su, S.-J.; Agata, Y.; Lan, H.; Kido, J. *Adv. Mater.* **2009**, *21*, 1271.
- (21) Mizuno, Y.; Takasu, I.; Uchikoga, S.; Enomoto, S.; Sawabe, T.; Amano, A.; Wada, A.; Sugizaki, T.; Yoshida, J.; Ono, T.; Adachi, C. *J. Phys. Chem. C* **2012**, *116*, 20681.
- (22) Wang, L.; Jiang, Y.; Luo, J.; Zhou, Y.; Zhou, J.; Wang, J.; Pei, J.; Cao, Y. *Adv. Mater.* **2009**, *21*, 4854.
- (23) Chien, C.-H.; Chen, C.-K.; Hsu, F.-M.; Shu, C.-F.; Chou, P.-T.; Lai, C.-H. *Adv. Funct. Mater.* **2009**, *19*, 560.
- (24) Zhu, M.; Wang, Q.; Gu, Y.; Cao, X.; Zhong, C.; Ma, D.; Qin, J.; Yang, C. *J. Mater. Chem.* **2011**, *21*, 6409.
- (25) Xiao, L.; Chen, Z.; Qu, B.; Luo, J.; Kong, S.; Gong, Q.; Kido, J. *Adv. Mater.* **2011**, *23*, 926.

- (26) Jeon, S. O.; Lee, J. Y. *J. Mater. Chem.* **2012**, *22*, 4233.
- (27) Zhao, J.; Xie, G.-H.; Yin, C.-R.; Xie, L.-H.; Han, C.-M.; Chen, R.-F.; Xu, H.; Yi, M.-D.; Deng, Z.-P.; Chen, S.-F.; Zhao, Y.; Liu, S.-Y.; Huang, W. *Chem. Mater.* **2011**, *23*, 5331.
- (28) McCarthy, M. A.; Liu, B.; Donoghue, E. P.; Kravchenko, I.; Kim, D. Y.; So, F.; Rinzler, A. G. *Science* **2011**, *332*, 570.
- (29) Son, H. S.; Seo, C. W.; Lee, J. Y. *J. Mater. Chem.* **2011**, *21*, 5638.
- (30) Jeong, S. H.; Lee, J. Y. *J. Mater. Chem.* **2011**, *21*, 14604.
- (31) Yang, W.; Zhang, Z.; Han, C.; Zhang, Z.; Xu, H.; Yan, P.; Zhao, Y.; Liu, S. *Chem. Commun.* **2013**, *49*, 2822.
- (32) Yu, D.; Zhao, F.; Han, C.; Xu, H.; Li, J.; Zhang, Z.; Deng, Z.; Ma, D.; Yan, P. *Adv. Mater.* **2012**, *24*, 509.
- (33) Sasabe, H.; Toyota, N.; Nakanishi, H.; Ishizaka, T.; Pu, Y.-J.; Kido, J. *Adv. Mater.* **2012**, *24*, 3212.
- (34) Cho, Y. J.; Lee, J. Y. *Adv. Mater.* **2011**, *23*, 4568.
- (35) Mondal, E.; Hung, W.-Y.; Dai, H.-C.; Wong, K.-T. *Adv. Funct. Mater.* **2013**, *23*, 3096.
- (36) Hsu, F.-M.; Chien, C.-H.; Shu, C.-F.; Lai, C.-H.; Hsieh, C.-C.; Wang, K.-W.; Chou, P.-T. *Adv. Funct. Mater.* **2009**, *19*, 2834.
- (37) Jeon, S. O.; Yook, K. S.; Joo, C. W.; Lee, J. Y. *Adv. Funct. Mater.* **2009**, *19*, 3644.
- (38) Chou, H.-H.; Cheng, C.-H. *Adv. Mater.* **2010**, *22*, 2468.
- (39) Gong, S.; Fu, Q.; Wang, Q.; Yang, C.; Zhong, C.; Qin, J.; Ma, D. *Adv. Mater.* **2011**, *23*, 4956.
- (40) Jeon, S. O.; Yook, K. S.; Joo, C. W.; Lee, J. Y. *Adv. Mater.* **2010**, *22*, 1872.
- (41) Shao, S.; Ding, J.; Ye, T.; Xie, Z.; Wang, L.; Jing, X.; Wang, F. *Adv. Mater.* **2011**, *23*, 3570.
- (42) Xiao, L. X.; Su, S.-J.; Agata, Y.; Lan, H.; Kido, J. *Adv. Mater.* **2009**, *21*, 1271.
- (43) Chaskar, A.; Chen, H.-F.; Wong, K.-T. *Adv. Mater.* **2011**, *23*, 3876.
- (44) Chen, J.; Shi, C.; Fu, Q.; Zhao, F.; Hu, Y.; Feng, Y.; Ma, D. *J. Mater. Chem.* **2012**, *22*, 5164.
- (45) Han, C.; Zhang, Z.; Xu, H.; Yue, S.; Li, J.; Yan, P.; Deng, Z.; Zhao, Y.; Yan, P.; Liu, S. *J. Am. Chem. Soc.* **2012**, *134*, 19179.
- (46) Jiang, W.; Duan, L.; Qiao, J.; Dong, G.; Wang, L.; Qiu, Y. *Org. Lett.* **2011**, *13*, 3146.
- (47) An, Z.-F.; Chen, R.-F.; Yin, J.; Xie, G.-H.; Shi, H.-F.; Tsuboi, T.; Huang, W. *Chem.—Eur. J.* **2011**, *17*, 10871.
- (48) Yook, K. S.; Lee, J. Y. *Adv. Mater.* **2012**, *24*, 3169.
- (49) Liu, H.; Cheng, G.; Hu, D.; Shen, F.; Lv, Y.; Sun, G.; Yang, B.; Lu, P.; Ma, Y. *Adv. Funct. Mater.* **2012**, *22*, 2830.
- (50) Cho, Y. J.; Lee, J. Y. *Chem.—Eur. J.* **2011**, *17*, 11415.
- (51) Fan, C.; Zhao, F.; Gan, P.; Yang, S.; Liu, T.; Zhong, C.; Ma, D.; Qin, J.; Yang, C. *Chem.—Eur. J.* **2012**, *18*, 5510.
- (52) Kim, D.; Salman, S.; Veaceslav, C.; Salomon, E.; Padmaperuma, A. B.; Sapochak, L. S.; Kahn, A.; Bredas, J.-L. *Chem. Mater.* **2010**, *22*, 247.
- (53) Han, C.; Xie, G.; Xu, H.; Zhang, Z.; Xie, L.; Zhao, Y.; Liu, S.; Huang, W. *Adv. Mater.* **2011**, *23*, 2491.
- (54) Yu, D.; Zhao, Y.; Xu, H.; Han, C.; Ma, D.; Deng, Z.; Gao, S.; Yan, P. *Chem.—Eur. J.* **2011**, *17*, 2592.
- (55) Cai, X.; Padmaperuma, A. B.; Sapochak, L. S.; Vecchi, P. A.; Burrows, P. E. *Appl. Phys. Lett.* **2008**, *92*, 083308.
- (56) Zhang, Z.; Zhang, Z.; Chen, R.; Jia, J.; Han, C.; Zheng, C.; Xu, H.; Yu, D.; Zhao, Y.; Yan, P.; Liu, S.; Huang, W. *Chem.—Eur. J.* **2013**, *19*, 9549.
- (57) Mamada, M.; Ergun, S.; Pérez-Bolívar, C.; Pavel Anzenbacher, J. *Appl. Phys. Lett.* **2011**, *98*, 073305.
- (58) Bin, J.-K.; Cho, N.-S.; Hong, J.-I. *Adv. Mater.* **2012**, *24*, 2911.
- (59) Han, C.; Zhang, Z.; Xu, H.; Li, J.; Xie, G.; Chen, R.; Zhao, Y.; Huang, W. *Angew. Chem., Int. Ed.* **2012**, *51*, 10104.
- (60) Gong, S.; Fu, Q.; Zeng, W.; Zhong, C.; Yang, C.; Ma, D.; Qin, J. *Chem. Mater.* **2012**, *24*, 3120.
- (61) Gong, S.; He, X.; Chen, Y.; Jiang, Z.; Zhong, C.; Ma, D.; Qin, J.; Yang, C. *J. Mater. Chem.* **2012**, *22*, 2894.
- (62) Sapochak, L. S.; Padmaperuma, A. B.; Vecchi, P. A.; Qiao, H.; Burrows, P. E. *Proc. of SPIE* **2006**, 6333, 63330F.
- (63) Sapochak, L. S.; Padmaperuma, A. B.; Cai, X.; Male, J. L.; Burrows, P. E. *J. Phys. Chem. C* **2008**, *112*, 7989.
- (64) Padmaperuma, A. *Proc. SPIE* **2009**, 7415, 74150H.
- (65) Han, C.; Zhao, Y.; Xu, H.; Chen, J.; Deng, Z.; Ma, D.; Li, Q.; Yan, P. *Chem.—Eur. J.* **2011**, *17*, 5800.
- (66) Han, C.; Xie, G.; Li, J.; Zhang, Z.; Xu, H.; Deng, Z.; Zhao, Y.; Yan, P.; Liu, S. *Chem.—Eur. J.* **2011**, *17*, 8947.
- (67) Han, C.; Xie, G.; Xu, H.; Zhang, Z.; Yu, D.; Zhao, Y.; Yan, P.; Deng, Z.; Liu, S. *Chem.—Eur. J.* **2011**, *17*, 445.
- (68) Han, C.; Zhang, Z.; Xu, H.; Li, J.; Zhao, Y.; Yan, P.; Liu, S. *Chem.—Eur. J.* **2013**, *19*, 1385.
- (69) Adachi, C.; Kwong, R. C.; Djurovich, P.; Adamovich, V.; Baldo, M. A.; Thompson, M. E.; Forrest, S. R. *Appl. Phys. Lett.* **2001**, *79*, 2082.
- (70) Méhes, G.; Nomura, H.; Zhang, Q.; Nakagawa, T.; Adachi, C. *Angew. Chem., Int. Ed.* **2012**, *51*, 11311.
- (71) Zhang, Q.; Li, J.; Shizu, K.; Huang, S.; Hirata, S.; Miyazaki, H.; Adachi, C. *J. Am. Chem. Soc.* **2012**, *134*, 14706.
- (72) Goushi, K.; Yoshida, K.; Sato, K.; Adachi, C. *Nat. Photon.* **2012**, *6*, 253.
- (73) Uoyama, H.; Goushi, K.; Shizu, K.; Nomura, H.; Adachi, C. *Nature* **2012**, *492*, 234.
- (74) Su, S.-J.; Gonmori, E.; Sasabe, H.; Kido, J. *Adv. Mater.* **2008**, *20*, 4189.
- (75) Swensen, J. S.; Polikarpov, E.; Von Ruden, A.; Wang, L.; Sapochak, L. S.; Padmaperuma, A. B. *Adv. Funct. Mater.* **2011**, *21*, 3250.
- (76) Han, C.; Zhang, Z.; Xu, H.; Xie, G.; Li, J.; Zhao, Y.; Deng, Z.; Liu, S.; Yan, P. *Chem.—Eur. J.* **2013**, *19*, 141.
- (77) Becke, A. D. *J. Chem. Phys.* **1993**, *98*, 5648.
- (78) Lee, C.; Yang, W.; Parr, R. G. *Phys. Rev. B* **1988**, *37*, 785.
- (79) Frisch, M. J.; Trucks, G. W.; Schlegel, H. B.; Scuseria, G. E.; Robb, M. A.; Cheeseman, J. R.; Montgomery, J. A., Jr.; T. V.; Kudin, K. N.; Burant, J. C.; Millam, J. M.; Iyengar, S. S.; Tomasi, J.; Barone, V.; Mennucci, B.; Cossi, M.; Scalmani, G.; Rega, N.; Petersson, G. A.; Nakatsuji, H.; Hada, M.; Ehara, M.; Toyota, K.; Fukuda, R.; Hasegawa, J.; Ishida, M.; Nakajima, T.; Honda, Y.; Kitao, O.; Nakai, H.; Klene, M.; Li, X.; Knox, J. E.; Hratchian, H. P.; Cross, J. B.; Adamo, C.; Jaramillo, J.; Gomperts, R.; Stratmann, R. E.; Yazyev, O.; Austin, A. J.; Cammi, R.; Pomelli, C.; Ochterski, J. W.; Ayala, P. Y.; Morokuma, K.; Voth, G. A.; Salvador, P.; Dannenberg, J. J.; Zakrzewski, V. G.; Dapprich, S.; Daniels, A. D.; Strain, M. C.; Farkas, O.; Malick, D. K.; Rabuck, A. D.; Raghavachari, K.; Foresman, J. B.; Ortiz, J. V.; Cui, Q.; Baboul, A. G.; Clifford, S.; Cioslowski, J.; Stefanov, B. B.; G. Liu, A. L.; Piskorz, P.; Komaromi, I.; L.Martin, R.; Fox, D. J.; Keith, T.; Al-Laham, M. A.; Peng, C. Y.; Nanayakkara, A.; Challacombe, M.; Gill, P. M. W.; Johnson, B.; Chen, W.; Wong, M. W.; Gonzalez, C.; Pople, J. A. *Gaussian 03*, Revision D.02; Gaussian Inc.: Pittsburgh, PA, 2004.
- (80) Wada, A.; Yasuda, T.; Zhang, Q.; Yang, Y. S.; Takasu, I.; Enomoto, S.; Adachi, C. *J. Mater. Chem. C* **2013**, *1*, 2404.
- (81) Kim, D.; Zhu, L.; Brédas, J.-L. *Chem. Mater.* **2012**, *24*, 2604.
- (82) Kim, D.; Coropceanu, V.; Brédas, J.-L. *J. Am. Chem. Soc.* **2011**, *133*, 17895.